Enhanced absorption of thin-film photovoltaic cells using an optical cavity

Enhanced absorption of thin-film photovoltaic cells using an optical cavity

Lee A. Weinstein,[1,†] Wei-Chun Hsu,[1,†] Selçuk Yerci,[1,2] Svetlana V. Boriskina,[1] and Gang Chen[1,*]

[1] *Department of Mechanical Engineering, Massachusetts Institute of Technology, Cambridge, MA 20036, USA*
[2] *Micro and Nanotechnology Programme, Middle East Technical University, Ankara,06800 Turkey*
[†]*Authors contributed equally to this work* **Corresponding author: gchen2@mit.edu*

We show via numerical simulations that the absorption and solar energy conversion efficiency of a thin-film photovoltaic (PV) cell can be significantly enhanced by embedding it into an optical cavity. A reflective hemi-ellipsoid with an aperture for sunlight placed over a tilted PV cell reflects unabsorbed photons back to the cell, allowing for multiple opportunities for absorption. Ray tracing simulations predict that with the proposed cavity a textured thin-film silicon cell can exceed the Yablonovitch (Lambertian) limit for absorption across a broad wavelength range, while the performance of the cavity-embedded planar PV cell approaches that of the cell with the surface texturing.

1. Introduction

Photovoltaics (PV) offer a promising answer to the challenge of a renewable energy future[1]. Even with significant progress in recent years, efforts are being made to reduce cost even further so that PV can reach parity with conventional fossil fuels without government subsidies[2]. One approach to cost reduction is using thin-film crystalline silicon (c-Si) PV cells, which use significantly less high-quality silicon material than traditional cells[3]. The silicon wafer typically accounts for 30% - 40% of the total PV module cost, and this cost can be reduced if less material is used[4,5].

The drawback of thin-film cells is that incident photons have a shorter travel distance through the material than in traditional cells, yielding a lower chance of being absorbed. Tiedje and Yablonovitch, et. al. established an absorptance limit for silicon PV cells as a function of cell thickness (the "Yablonovitch limit" or "Lambertian limit")[6]. This absorptance limit can be combined with the Shockley-Queisser limit (for example) to predict a solar to electricity conversion efficiency limit[7]. Absorptance in the Yablonovitch limit assumes incident photons are perfectly coupled (100% transmittance) into the cell and scattered isotropically at the front and back surfaces of the cell. Photons which would otherwise escape from the cell are trapped inside the cell if they have been scattered into an angle exceeding the critical angle (total internal reflection). This results in longer photon path lengths through the cell and therefore higher chance of absorption[8]. The absorption limit A is given by:

$$A(\lambda) = \frac{\alpha(\lambda)L}{\alpha(\lambda)L + \frac{1}{F}} \quad (1)$$

where $\alpha(\lambda)$ is the wavelength dependent absorption coefficient of the PV material, L is the cell thickness, and F is the absorption enhancement factor. The absorption enhancement factor is $4n^2$ in the Yablonovitch limit, where n is the PV refractive index. Substituting this into Eq. (1) yields the familiar form of the Yablonovitch limit:

$$A(\lambda) = \frac{\alpha(\lambda)}{\alpha(\lambda) + \frac{1}{4n^2 L}} \quad (2)$$

There is also a lower 2D absorption limit for surfaces which only scatter in one dimension. In this case, the absorption enhancement factor is πn rather than $4n^2$[9].

Most strategies for enhancing thin-film cell absorption pursued up to this point have used cell surface texturing to scatter photons into a wider range of angles into the cell with the aim of approaching the Yablonovitch limit[10–14]. However, the PV cell efficiency can also be increased by limiting the angular range through which photons (both trapped and emitted in the process of radiative recombination) can escape the cell[15–18]. For angle limited PV cells, the maximum absorption enhancement factor is increased from $4n^2$ to $4n^2/\sin^2\theta$ where θ is the half-angle of the absorption cone of the PV cell[19,20]. In this paper we investigate the use of an external optical cavity to improve absorption of light in thin-film silicon PV cells both with and without surface texturing via the angular selectivity mechanism.

2. Hemi-ellipsoidal Optical Cavity

The optical cavity investigated is an ellipsoidal dome with a reflective coating and a small aperture allowing sunlight to reach the cell, as shown in Fig. 1. Similar cavities have been shown to reduce radiative recombination emission losses in PV cells[21] and thermal emission losses in thermal systems[22,23]. Here, we show how it can also increase absorption in thin film PV cells. If the cell is slightly tilted, some of the photons that are not absorbed and leave the PV cell after bouncing off its back reflector can now be trapped inside the cavity. Owing to its ellipsoidal shape, the cavity reflects these photons back to the PV cell, which allows for more opportunities for absorption and effectively increases absorptance of the cell.

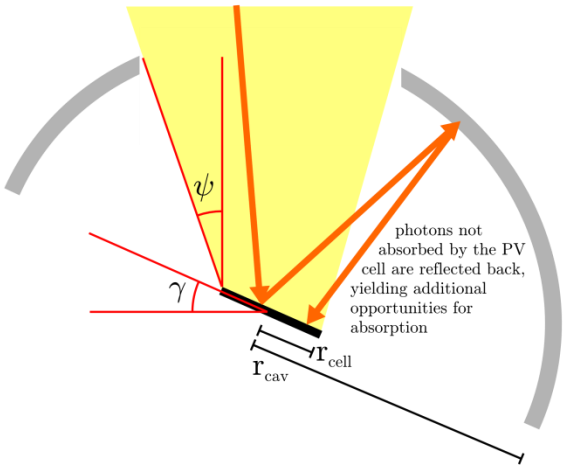

Figure 1 Diagram of the PV cell cavity enhancement concept. Sunlight incident on a tilted cell that is not absorbed is reflected back to the cell, yielding more opportunities for absorption. Important geometric parameters include: aperture acceptance angle ψ, cell tilt angle γ, cell radius r_{cell}, and cavity radius r_{cav}.

The geometry of the cavity is an oblate ellipsoid, with the relationship between the semi-major axis r_{cav} ("radius" of the ellipsoid) and semi-minor axis h ("height" of the ellipsoid) given by

$$r_{cav} = \sqrt{h^2 + r_{cell}^2} \tag{3}$$

where r_{cell} is the radius of the PV cell in the cavity. This geometry is used because it ensures that any ray originating from the PV cell which is specularly reflected from the ellipsoidal cavity will return to the PV cell[24,25]. The ellipsoid is tilted along with the cell such that its minor axis remains orthogonal to the PV cell, in order to preserve the previously mentioned geometrical reflecting property. Slight variations to this configuration (e.g., ellipsoid minor axis aligned with incident sunlight, a hemispherical cavity, etc.) were investigated and found to have marginally lower performance, so the results for those studies will not be reported here.

Cavity performance is predicted using ray tracing, which is a Monte Carlo technique that can be used to evaluate the radiative properties of systems[26]. Rays representing incident solar radiation are incident on the PV cell, with location and incidence angle determined by randomly generated numbers and the appropriate weighting functions. Based on the cell absorptance, the rays have a chance of being absorbed or reflected specularly (our optical simulations detailed below show that higher order surface diffractions are negligible for the investigated structured surfaces, see Appendix A). The rays are propagated through the cavity until all rays have been absorbed by the cell ("absorbed"), absorbed by the cavity walls ("mirror losses"), lost through the aperture ("aperture losses") or absorbed by the cavity floor ("floor losses"). The effective absorptance A of the cell embedded into the cavity is given simply by

$$A = \frac{N_{cell}}{N_{inc}} \cos\gamma \tag{4}$$

where N_{cell} is the number of rays absorbed at the cell, N_{inc} is the total number of rays incident on the cell, and γ is the tilt angle. The $\cos\gamma$ term accounts for effective area losses due to the incident sunlight not being normal to the cell.

There are three primary geometric parameters of the cavity to optimize for achieving high absorption and energy conversion efficiency: the acceptance angle of the cavity aperture, the tilt angle of the PV cell, and the size ratio of the cavity radius to the PV cell radius (all shown in Fig. 1). Another important cavity parameter is the wall specular reflectance, which is assumed to be 95%, a value which is achievable in the relevant spectral range using conventional metal coatings[27].

The cavity aperture acceptance angle, defined as the angle between a line from the edge of the PV cell to the near edge of the aperture and a normally incident ray from the sun, determines the maximum solar concentration ratio achievable at the cell[28]. It should be noted that this cavity aperture acceptance angle (shown in Fig. 1 as ψ) is different from the acceptance angle typically used in CPV applications, which refers to the tolerance of concentrating optics to misalignment. Larger cavity acceptance angles allow for higher concentration ratios but reduce the cavity effectiveness by allowing more photons to escape through the aperture. A fixed acceptance angle of 5° is used in this study, which allows for moderate concentration ratios (up to 360 suns).

Tilt angle is an important parameter to consider because if the cell is not tilted then most photons reflected from the cell leave the cavity through the aperture, but if the cell is tilted too steeply then the projected area of the cell in the direction of the incident sunlight becomes small. The maximum tilt angle to consider is the smallest angle such that no photons coming through the aperture are reflected directly back toward the aperture. This maximum tilt angle γ_{max} can be given by (see Appendix B for derivation)

$$\gamma_{max} = \psi + sin^{-1}\left(\frac{r_{cell}}{r_{cav}}\right) \tag{5}$$

where r_{cell} and r_{cav} are the radii of the cell and cavity respectively, and ψ is the aperture acceptance angle. This max angle is not necessarily optimal, as shallower angles resulting in lower cosine losses may outweigh the additional aperture losses. To find an optimum value for the tilt angle, in Fig. 2 we plot the effective absorptance of a cell with an absorptance of 0.5 and varied tilt angle. As expected, effective absorptance increases with tilt angle as aperture losses are reduced until the optimal angle, after which performance degrades due to cosine losses. The maximum tilt angle of 16.5° predicted by Eq. (5) is marked by the dashed vertical line, and in this case the optimal angle is slightly smaller, about 14.5°. It is worth noting that other absorptance values besides 0.5 can be used to optimize the geometric parameters, and the difference in results is negligible for a wide range of absorptances.

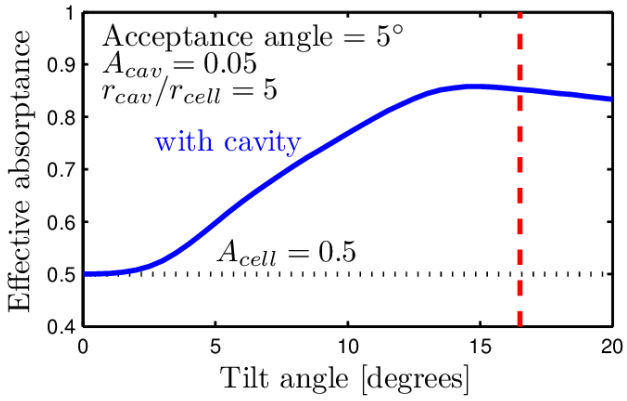

Figure 2 Effective absorptance of a cell within a cavity as a function of the cell tilt angle. The dotted black line at 0.5 shows the absorptance of the cell in the absence of the cavity. The vertical dashed red line denotes the maximum tilt angle of 16.5° given by Eq. (5), while the optimal angle is about 14.5°.

Cavity size ratio (the ratio of cavity radius to cell radius) is also important to consider for maximizing cell absorption. Figure 3 shows the fractions of the rays initially reflected from a cell with absorptance of 0.5, which – after bouncing within the cavity – are (i) absorbed by the cell, (ii) absorbed by the cavity and (iii) lost through the aperture. There is an optimal size ratio, as very small cavities require large apertures to maintain a decent concentration ratio (leading to large aperture losses), while large elliptical cavities focus the rays back out of the aperture in only one reflection off the cell. It can be noted that larger size ratios call for shallower tilt angles and therefore lower cosine losses, an advantage not reflected in Fig. 3. It should also be noted that these results use the tilt angle given by Eq. (5), so slightly improved performance could be obtained by finding the optimal angle at each cavity size ratio.

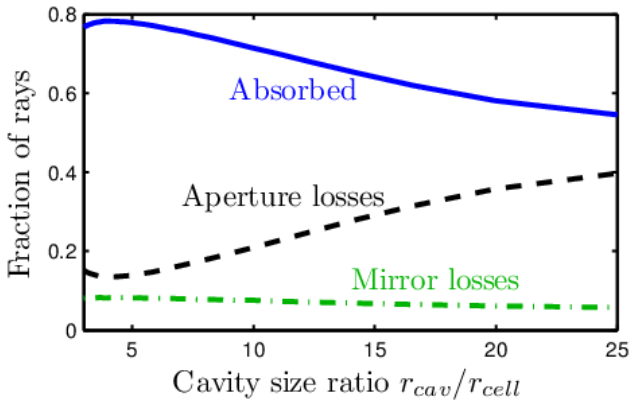

Figure 3 Fraction of rays which absorbed by the cell ("absorbed"), absorbed by the cavity ("mirror losses") and lost through the aperture ("aperture losses") as a function of cavity size ratio. The cell absorptance is taken as 0.5, and the tilt angle used is given by Eq. (5).

3. Absorption Enhancement of Thin-Film PV

To calculate how much the cavity enhances the effective absorptance of the embedded PV cell, we fixed the cavity geometry and ran ray tracing simulations for cell absorptances varying from 0 to 1 (Fig. 4b). The cavity parameters used for the results in Fig. 4b (and hereafter) were as follows: an acceptance angle of 5°, a cavity specular reflectance of 95%, a cavity size ratio of 5, and a cell tilt angle of 14.5°. As can be seen in Fig. 4b, the largest enhancements occur for moderate absorptances in the range of ~0.2 – 0.7. The enhancement is small for low cell absorptances because even with additional opportunities for absorbing incident photons, the photons are still more likely to be reflected away from the cell and either escape or get absorbed elsewhere in the cavity. The enhancement is small for high absorptances because almost all the photons are absorbed on the initial incidence on the cell, so there are few additional photons left to absorb with the aid of the cavity. It is also worth noting that for absorptances very close to 1 the cavity actually lowers the cell performance, as the cosine losses from the tilted cell outweigh the advantage of increased absorptance of incident photons.

In order to calculate the absorptance of a PV cell without a cavity, the wave optics module in COMSOL Multiphysics was used to simulate the PV cell optical response including cell reflectance and absorptance for both transverse electric (TE) and transverse magnetic (TM) polarizations. Three types of c-Si PV cell were studied, including unpatterned (planar) thin-film cells and cells with either a three dimensional (3D) pattern of inverted nano-pyramids (INPs) or a two dimensional (2D) pattern of parallel periodic grooves. Silicon nitride antireflection layers with thicknesses of 70 nm and 100 nm were placed on top of the planar and textured silicon layers, respectively. The periodicities for both the 2D grooves and 3D INPs are 700 nm. For textured solar cells, an unavoidable planar area between each repeating unit cell forms a ridge region, which can be seen in Fig. 4a, and this ridge separation is set to be 50 nm[10]. Floquet periodic boundary conditions are implemented on the sides of the computation window, and a perfect electric conductor (PEC) boundary condition is used to mimic the effect of a back mirror for the PV cell. The 2D grooved solar cells have 200nm-thick oxide and 600nm-thick silver on the back of the silicon. For the 3D inverted pyramids, we assumed a PEC boundary condition directly underneath the silicon layer to improve numerical accuracy and reduce computation time. Absorptance for varying incidence angles from normal to 20° were calculated (capturing the majority of ray incidence angles), however no significant angular dependence was observed in this range.

Since photons absorbed in parts of the cell other than the silicon (e.g., the nitride layer) are not useful, effective absorptance of the cell A_{eff} with the cavity (for a particular wavelength) is given by

$$A_{eff} = \frac{A_{Si}}{A_{tot}} F(A_{tot}) \qquad (6)$$

where A_{Si} is the absorptance of the silicon portion of the cell, A_{tot} is the total absorptance of the cell and F is the function which gives the cavity enhancement (i.e., the

solid blue curve in Fig. 4b). Applying Eq. (6) to the spectral absorptance curve of a solar cell yields the enhancement with the cavity, as shown in Fig. 4c for a 5 μm thick planar c-Si cell. There is significant absorption enhancement in wavelength range of 700 – 1000 nm, as the cell by itself has moderate absorption values in this range. For the range of 450 – 700 nm, the enhancement is small, as the bare cell already absorbs effectively in this range.

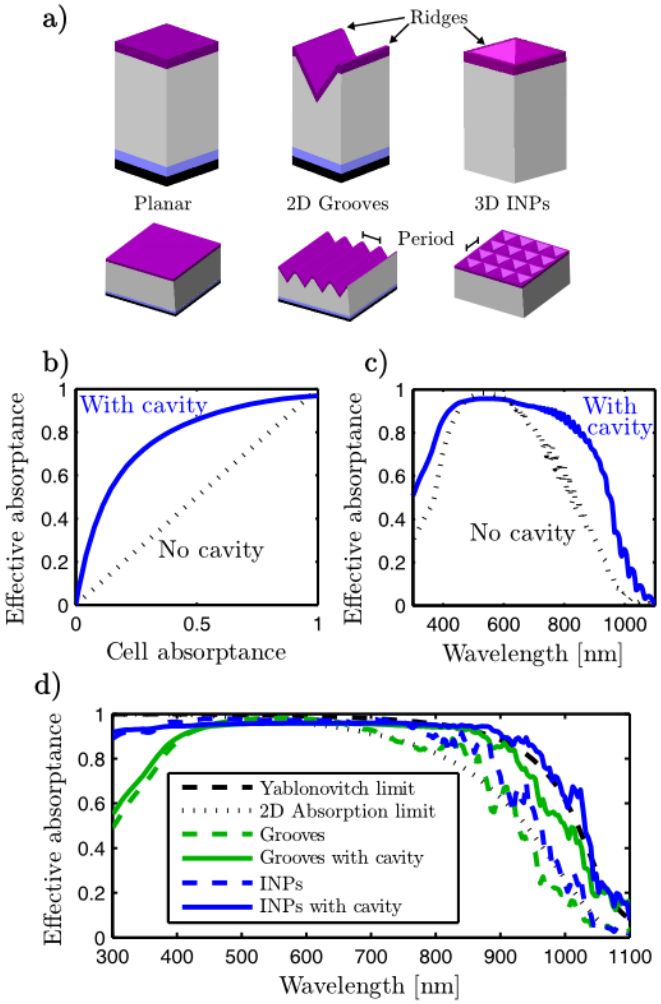

Figure 4 (a) The schematic of simulated planar, 2D grooved, and 3D INPs solar cells: the layers shown in purple, gray, blue and black represent antireflective silicon nitride, silicon, silicon dioxide and silver, respectively. (b) Effective absorptance of cell within a cavity as a function of cell absorptance (solid blue curve) with cell performance in absence of cavity for comparison (dotted black curve). (c) Spectral absorptance of a 5 μm thick planar silicon cell with (solid blue curve) and without the cavity (dotted black curve). (d) Spectral absorptance for 5 μm silicon cells within a cavity (solid curves) and without a cavity (dashed curves). Surface patterns shown are grooved surface (green curves) and inverted nano-pyramids (INPs, blue curves). The Yablonovitch limit (dashed black curve) and 2D absorption limit (dotted black curve) are shown for comparison.

The absorptance enhancement spectrum for 5 μm c-Si cells with surface patterning (grooves and inverted nano-pyramids) is shown in Fig. 4d, along with the Yabolonovitch absorption limit for comparison. For the cell with the grooved surface, the introduction of the cavity brings performance close to the Yablonovitch limit, while the cell with the inverted nano-pyramids and cavity exceeds the Yablonovitch limit for wavelengths greater than 800 nm. It should be emphasized that photons with the energies in this spectral range close to the bandgap of silicon can be converted most efficiently by Si PV cells. The angle-limited absorption limit is not plotted here (which the proposed cavity would never be able to exceed) as for our cavity's acceptance angle the absorptance would effectively be unity across the entire spectral range.

To quantify how cavity-enhanced absorptance affects PV cell performance, we calculate the photo-generated current density, J_{ph}, and the cell efficiency. Both of these quantities are calculated assuming a solar concentration of 25, chosen because such an optical concentration captures all the sunlight that would be incident on the cavity ($r_{cav}/r_{cell} = 5$). The photo-generated current density can be modeled by assuming that every absorbed photon in the silicon with energy above the bandgap excites one electron-hole pair. The AM1.5D solar spectrum[29] is used, as the cavity-embedded cell is expected to be operated under concentrated sunlight illumination. Efficiency can be calculated using a simple 1D model, with the current density J calculated as:

$$J = J_o[exp(qV/kT) - 1] - J_{ph} \quad (7)$$

where J_o is dark current density, q is elementary charge, V is voltage, k is the Boltzmann constant, and T is cell temperature, with proper silicon properties[30,31]. Efficiencies are calculated assuming p-type cell doping level of 10^{16}cm^{-3}, 500nm-thick n-type junction on the top surface with doping level of 10^{19}cm^{-3}, and surface recombination velocities of 30cm/s at both top and bottom surfaces. Figure 5a shows photo-generated current density and efficiency of planar, grooved, and inverted nano-pyramid (INP) patterned cells with and without the cavity as a function of the cell thickness. The photo-generated current density obtained using the Yablonovitch limit of absorption is shown for comparison.

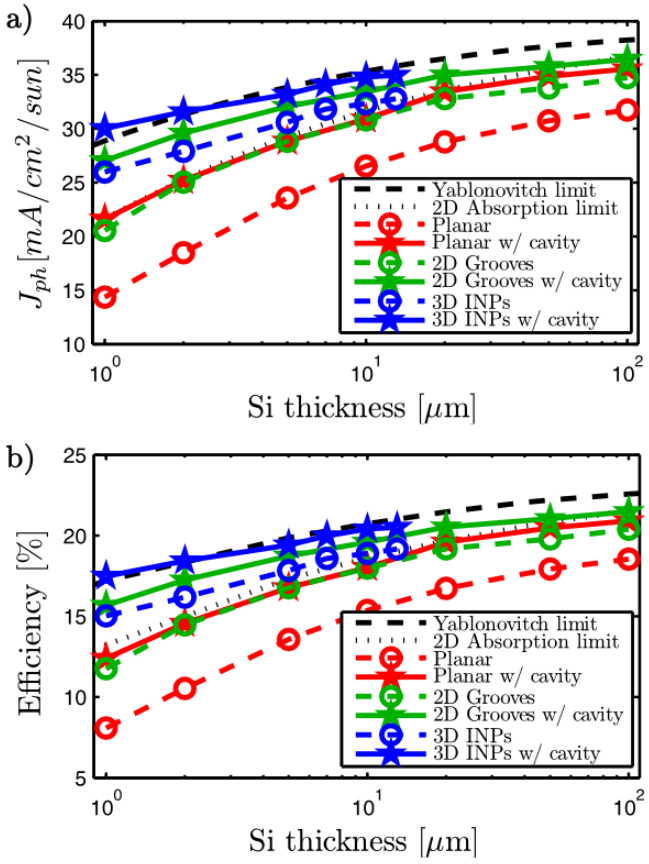

Figure 5 (a) Photo-generated current density and (b) efficiency as a function of cell thickness for planar (red), 2D grooved (green) and 3D INP (blue) surfaces both with (solid curves with pentagrams) and without the cavity (dashed curves with open circles). The photo-generated currents and efficiencies assuming the Yablonovitch limit (dashed black curve) and 2D limit (dotted black curve) for the cell absorptance are shown for comparison.

The photo-generated current density enhancement is most pronounced for planar cells, with improvements of about 7 mA/cm²/sun for very thin cells, and of about 5 mA/cm²/sun for conventional cells with thicknesses of 100μm and above. Planar cells have moderate absorption for a wide range of wavelengths, and thus benefit most from the cavity effect. The enhancement is less dramatic for patterned cells, as they already have fairly good absorptance, however there is still a significant improvement of around 5 mA/cm² for thin cells and 2 – 3 mA/cm² for thicker cells. The enhancement is significant enough that for INP patterned cells of < 2 μm in thickness, the cavity effect pushes the PV photo-generated current above the Yablonovitch limit. The performance of INP patterned cells is only plotted for cells with up to 13 μm thickness due to computational limitations for 3D COMSOL simulations. INP performance is expected to approach grooved cell performance at large thicknesses, as the increased scattering gives diminishing returns for thicker cells, and this trend is already noticeable for the thicknesses shown in Fig. 5. It is also worth noting that the planar cell with the cavity outperforms the grooved cell without the cavity, indicating that use of the cavity as a light trapping strategy achieves PV cell performance improvement comparable to that achieved via surface texturing. The trends for the efficiency results, which are shown in Fig 5b, closely mirror what was discussed for photo-generated current.

4. Conclusion

While prior research efforts have focused primarily on surface patterning of solar cells to enhance light trapping, the results reported here show that the proposed optical cavity can also lead to significant absorptance enhancements. This offers an alternative path to improve thin-film PV cell absorptance, which can be pursued either in parallel with surface patterning or separately. Modeling shows that the optical cavity used in conjunction with patterned PV cells can even exceed the Yablonovitch limit for absorption, especially for ultrathin (<2μm) solar cells. The effect of the cavity can be even stronger for thin film PV cells with higher radiative recombination emission rates (such as GaAs), as the cavity-imposed emission angular selectivity also enables re-cycling of emitted photons[16,21].

Acknowledgements

This work was funded by the DOE SunShot Initiative award DE- EE0005320 (PV cell simulations) and by the DOE EFRC S3TEC Center award DE-SC0001299/DE-FG02-09ER46577 (angular selectivity concept) The authors also thank Jiun-Yin Kuan for assistance with illustrations for figure 4a.

Appendix A – Results showing higher order refractions are negligible

COMSOL simulations can be used to calculate refraction from the surface of a patterned reflector, such as the PV cells investigated in this paper. The reflectance of the 0th, 1st and 2nd order refractions for unpolarized light at a 15° incidence angle on a 10 μm thick cell with a 2D groove pattern is shown in Fig. A1. As can be seen from the plot, the great majority of the contribution to reflectance comes from the 0th order reflection. This was found to be the case for other incidence angles and cell thicknesses as well.

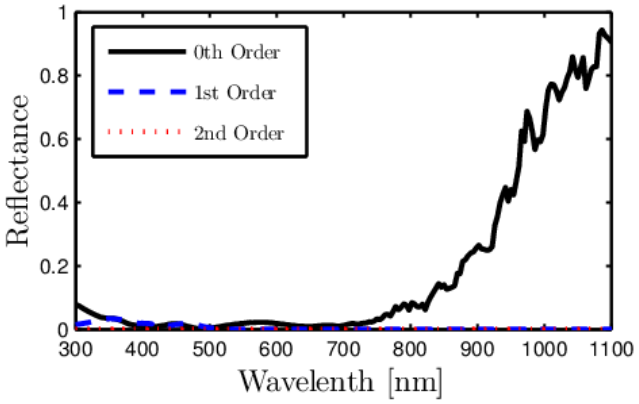

Figure A1 Reflectances for the 0th (solid black curve), 1st (dashed blue curve) and 2nd order (dotted red) diffractions from a 10 μm

thick silicon PV cell at 15° incidence angle as computed by COMSOL

Appendix B – Derivation of equation (5)

In order to derive Eq. (5) it is useful to define geometric parameters with respect to the PV cell, as shown in Fig. B1. In this figure, the lines normal to the incident sunlight (dotted green) intersect the lines normal to the PV cell (solid red) at the tilt angle γ. If the cell is tilted clockwise, the last ray to be captured in the cavity is at the acceptance angle ψ relative to the normal incidence sunlight. This last ray is labeled "A" in Fig. B1. When it reflects from the PV cell, it forms an angle $\gamma - \psi$ relative to the line normal to the PV cell, this reflected ray is labeled "B" and should hit the edge of the aperture. The edge of the aperture is defined by the opposite side of the PV cell, and the line between the edge of the aperture and PV cell (labeled "C") should be at the acceptance angle ψ relative to the normal incidence sunlight.

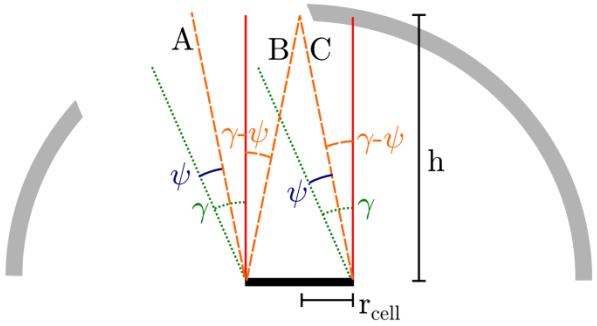

Figure B1 Diagram of cavity with the PV cell taken as horizontal. Lines and angles important to the derivation of Eq. (5) are marked.

Thus, lines from both edges of the PV cell to the edge of the aperture form the same angle with the lines normal to the PV cell: $\gamma - \psi$. This symmetry indicates that this edge of the aperture is at the apex of the hemi-ellipsoidal cavity, at a height of h. The distance between the edges of the PV cell and the apex of the dome is given by the Pythagorean theorem as $\sqrt{r_{cell}^2 + h^2}$. By applying Eq. (3), we can see that the distance is simply the semi-major axis of the ellipsoidal cavity r_{cav}. This sets up a simple trigonometric equation

$$sin(\gamma - \psi) = \frac{r_{cell}}{r_{cav}} \qquad \text{(B.1)}$$

which when rearranged for the tilt angle γ yields the form shown in Eq. (5).

References

[1] Epia E P I A 2013 Global Market Outlook for Photovoltaics 2013-2017 *Europe* 74

[2] Branker K, Pathak M J M and Pearce J M 2011 A review of solar photovoltaic levelized cost of electricity *Renew. Sustain. Energy Rev.* **15** 4470–82

[3] Green M a. 2007 Thin-film solar cells: review of materials, technologies and commercial status *J. Mater. Sci. Mater. Electron.* **18** 15–9

[4] Powell D M, Winkler M T, Choi H J, Simmons C B, Needleman D B and Buonassisi T 2012 Crystalline silicon photovoltaics: a cost analysis framework for determining technology pathways to reach baseload electricity costs *Energy Environ. Sci.* **5** 5874

[5] Forstner H, Bandil S, Zwegers M, Bollen R, Coletti G, Sinke W, Bultman J, Wyers P, Wertz R, Wu S, Lin K, Metz A, Moritz M, Markus Fischer Thomas Spiess M M, Mette A, Petter K, Gerlach A, Engelhart P, Xing G, Demenik A, McMullen D, Mohr C, Stassen A, Slufcik J, Yong L, Kaufmann S, Wan Y, Wang Y, Liu S, Richter A, Pai R, Wang K, Chen B, Luan A, Buchovskaja I, Spill B, Pingel R, Ramakrishnan A, Julsrud S, Osborne W, Flores A, Fath P, Nussbaumer H, Raithel S, Pingel S, Frank O, Zhu J, Ristow A, Oberbeck L and Demenik G 2014 *International Technology Roadmap for Photovoltaic (ITRPV) 2013 Results*

[6] Tiedje T, Yablonovitch E, Cody G D and Brooks B G 1984 Limiting efficiency of silicon solar cells *IEEE Trans. Electron Devices* **31** 711–6

[7] Shockley W and Queisser H J 1961 Detailed Balance Limit of Efficiency of p-n Junction Solar Cells *J. Appl. Phys.* **32** 510

[8] Green M A 2002 Lambertian light trapping in textured solar cells and light-emitting diodes: analytical solutions *Prog. Photovoltaics Res. Appl.* **10** 235–41

[9] Wang K X, Yu Z, Liu V, Raman A, Cui Y and Fan S *No Title*

[10] Mavrokefalos A, Han S E, Yerci S, Branham M S and Chen G 2012 Efficient light trapping in inverted nanopyramid thin crystalline silicon membranes for solar cell applications. *Nano Lett.* **12** 2792–6

[11] Han S E and Chen G 2010 Toward the Lambertian limit of light trapping in thin

nanostructured silicon solar cells. *Nano Lett.* **10** 4692–6

[12] Wang K X, Yu Z, Liu V, Cui Y and Fan S 2012 Absorption enhancement in ultrathin crystalline silicon solar cells with antireflection and light-trapping nanocone gratings. *Nano Lett.* **12** 1616–9

[13] Jeong S, Wang S and Cui Y 2012 Nanoscale photon management in silicon solar cells *J. Vac. Sci. Technol. A Vacuum, Surfaces, Film.* **30** 060801

[14] Jeong S, McGehee M D and Cui Y 2013 All-back-contact ultra-thin silicon nanocone solar cells with 13.7% power conversion efficiency. *Nat. Commun.* **4** 2950

[15] Kosten E D 2014 Optical designs for improved solar cell performance

[16] Kosten E D, Atwater J H, Parsons J, Polman A and Atwater H A 2013 Highly efficient GaAs solar cells by limiting light emission angle *Light Sci. Appl.* **2** e45

[17] Bermel P, Luo C, Zeng L, Kimerling L C and Joannopoulos J D 2007 Improving thin-film crystalline silicon solar cell efficiencies with photonic crystals *Opt. Express* **15** 16986

[18] Ulbrich C, Fahr S, Üpping J, Peters M, Kirchartz T, Rockstuhl C, Wehrspohn R, Gombert A, Lederer F and Rau U 2008 Directional selectivity and ultra-light-trapping in solar cells *Phys. status solidi* **205** 2831–43

[19] Yu Z, Raman A and Fan S 2010 Fundamental limit of light trapping in grating structures. *Opt. Express* **18 Suppl 3** A366–80

[20] Yu Z, Raman A and Fan S 2010 Fundamental limit of nanophotonic light trapping in solar cells. *Proc. Natl. Acad. Sci. U. S. A.* **107** 17491–6

[21] Braun A, Katz E A, Feuermann D, Kayes B M and Gordon J M 2013 Photovoltaic performance enhancement by external recycling of photon emission *Energy Environ. Sci.* **6** 1499

[22] Gordon J M, Feuermann D, Huleihil M and Katz E A 2004 New optical systems for the solar generation of nanomaterials *Optical Science and Technology, SPIE's 48th Annual Meeting* ed R Winston (International Society for Optics and Photonics) pp 99–108

[23] Weinstein L, Kraemer D, McEnaney K and Chen G 2014 Optical cavity for improved performance of solar receivers in solar-thermal systems *Sol. Energy* **108** 69–79

[24] Weinstein L A 2013 *Improvements to solar thermoelectric generators through device design* (Massachusetts Institute of Technology)

[25] Luque A and Araújo G 1990 *Physical limitations to photovoltaic energy conversion* (Bristol: Adam Hilger)

[26] Howell J R 1998 The Monte Carlo Method in Radiative Heat Transfer *J. Heat Transfer* **120** 547

[27] Johnson P B and Christy R W 1972 Optical Constants of the Noble Metals *Phys. Rev. B* **6** 4370–9

[28] Winston R, Minano J C, Benitez P G, Shatz N and Bortz J C 2005 *Nonimaging Optics* (Burlington, MA: Elsevier Academic Press)

[29] Standard A 2008 G173, Standard Tables for Reference Solar Spectral Irradiances: Direct Normal and Hemispherical on 37 Tilted Surface *Annu. B. ASTM Stand.*

[30] Green M A 1982 *Solar cells: Operating principles, technology, and system applications* vol 1, ed W R Bowen B A Brown (University of New South Wales)

[31] Sze S M and Ng K K 2007 Physics of Semiconductor Devices, 3rd Edition - Simon M. Sze, Kwok K. Ng *Physics of Semiconductor Devices, 3rd Edition.; John Wiley & Sons, Inc.; NJ* pp 164, 682